Estimating Information Exchange Performance of Engineered Cell-to-cell Molecular Communications: a Computational Approach

Colton Harper*, Massimiliano Pierobon*, and Maurizio Magarini‡
*Department of Computer Science and Engineering
University of Nebraska-Lincoln, Lincoln, Nebraska 68588 USA
‡Dipartimento di Elettronica, Informazione e Bioingegneria
Politecnico di Milano, I-20133 Milano, Italy
Email: charper@cse.unl.edu, pierobon@cse.unl.edu, maurizio.magarini@polimi.it

***Abstract*—Biological cells naturally exchange information for adapting to the environment, or even influencing other cells. One of the latest frontiers of synthetic biology stands in engineering cells to harness these natural communication processes for tissue engineering and cancer treatment, amongst others. Although experimental success has been achieved in this direction, approaches to characterize these systems in terms of communication performance and their dependence on design parameters are currently limited. In contrast to more classical communication systems, information in biological cells is propagated through molecules and biochemical reactions, which in general result in nonlinear input-output behaviors with system-evolution-dependent stochastic effects that are not amenable to analytical closed-form characterization. In this paper, a computational approach is proposed to characterize the information exchange in these systems, based on stochastic simulation of biochemical reactions and the estimation of information-theoretic parameters from sample distributions. In particular, this approach focuses on engineered cell-to-cell communications with a single transmitter and receiver, and it is applied to characterize the performance of a realistic system. Numerical results confirm the feasibility of this approach to be at the basis of future forward engineering practices for these communication systems.**

***Index Terms*—Molecular Communication; Synthetic Biology; Mutual Information; Stochastic Simulation**

I. Introduction

Cell signaling refers to the way individual biological cells and cell populations perceive, elaborate, and exchange biochemical information [25]. Through cell signaling, cells can adapt their behavior to determinate environmental conditions, or even influence how other cells behave, *i.e.*, cell-to-cell communication. Examples of cell-to-cell communication in nature include stem cell differentiation in tissues, the coordination of immune system response, bacteria biofilm formation and coordinated launch of infections, and the conception of bioluminescence [27]. The possibility of engineering cell-to-cell communication systems is at the cutting edge of the emerging discipline of synthetic biology, where these cellular communication abilities are harnessed and modified to control the propagation of information messages in biological environments, for applications ranging from controlled cell patterning for tissue engineering, to amorphous computing [3,26,28,35,40,42].

Currently, the most studied engineered cell-to-cell communication systems in synthetic biology can be classified as follows [28]: *short range communications*, which include communication via cell-cell contact [23], *medium range communications*, which include communication through virus-like particles, exosomes, or metabolic wiring [26], *long range communications*, which include communication through small molecule diffusion, such as those based on LuxR-LuxI and quorum sensing systems [40], or more recently based on Phloretin [41]. Despite these advances in experimentally demonstrating the capabilities of engineered cell-to-cell communications, this field would greatly benefit from the forward engineering principles of communication theory [22].

In this direction, the recent field of Molecular Communication (MC) has emerged from the communication engineering community to study information exchange at the nanoscale through the transmission, propagation, and reception of molecules [1,12]. The MC community has been recently focusing on biological cell communications, with the future goal of realizing a fully interconnected cyber-biological networking environment [2]. In particular, while the analysis of information capacity has mainly focused on single elements of cell communications, such as ligand-receptor binding [36], complete engineered cell-to-cell communications have been mainly considered for theoretical input-output models, such as the minimal engineered systems for analog communications analyzed in [29], or for digital-like communications in [37]. Other recent contributions include the design of components for potentially enhancing cell-to-cell communication through the design of information encoder [19] and decoder [20] inspired by classical communication engineering but implemented through synthetic biology tools. Despite these first results, there is currently a gap between the experimental reality in synthetic biology and the MC field. The highly nonlinear nature of engineered cell-to-cell communication systems, and the complexity of the noise sources in the biochemical reactions underlying the time evolution of a biological system, have

978-1-5386-4128-6/18/$31.00 ©2018 IEEE

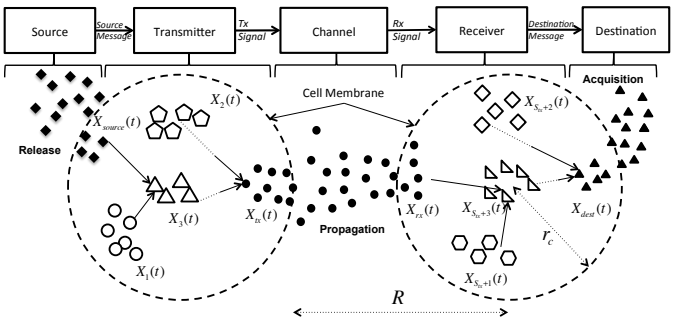

Fig. 1: Scheme of engineered cell-to-cell molecular communication systems considered in this paper.

encouraged MC researchers to adopt strong assumptions to apply classical communication engineering tools and models.

In this paper, we abstract the main features of engineered cell-to-cell communication systems, and demonstrate through an analytical formulation that in general communication models of these systems do not have analytical solutions in terms of input-output behavior, and their stochastic components are not analytically tractable to characterize the communication performance of the system with closed-form formulas. As a consequence, we propose a computational approach based on chemical stochastic simulation tools and estimation of information-theoretic parameters from sample distributions. Additionally, we apply the proposed method to a realistic engineered cell-to-cell communication system based on the LuxR-LuxI cell communication modules, where the synthetic biology components are derived from the artificial sender and receiver design included in the experimental work in [30]. We estimate the mutual information of this system in terms of bits per message as function of the probability distribution of the input information.

The remainder of this paper is organized as follows. In Sec. II, we abstract the main features of an engineered cell-to-cell molecular communication system, as well as list the main assumptions at the basis of the models discussed in this paper. In Sec. III, we present the formulation of the proposed methodology to characterize the performance of an engineered cell-to-cell communication system, while in Sec. IV we describe a realistic case study and the main elements of its computational model. Numerical results in terms of Mutual Information (MI) for the system under analysis are discussed in Sec. V. Finally, in Sec. VI we conclude the paper.

II. Engineered Cell-to-cell Molecular Communication System Model

The reference model of the engineered cell-to-cell communication system considered in this paper is shown in Fig. 1. In this model, a *Source Message* is released in the environment where the cells live by the information Source, it is processed by the Transmitter cell through a series of chained chemical reactions into a transmitted signal (*Tx Signal*), which is delivered to the Receiver cell, where it is processed by another series of chained chemical reactions into a *Destination Message* that is acquired by the Destination. In particular, the chemical reactions at the transmitter cell transduce the source message $X_{source}(t)$, as function of the time t, into concentrations of molecules of different species $X_i(t)$, $i = 1, \ldots, S_{tx}$, with the final effect of shaping (*e.g.*, filtering, amplification) the concentration of transmitted molecules $X_{tx}(t)$ ($= X_{S_{tx}}(t)$ at the transmitter) according to the message. Similarly, the chemical reactions at the receiver cell transduce the concentration of received molecules $X_{rx}(t)$ ($= X_{S_{rx}}(t)$ at the receiver) into concentrations of molecules of different species $X_j(t)$, $j = S_{tx}+1, \ldots, S_{tx}+S_{rx}$, to shape the destination message $X_{dest}(t)$. The nature of the source message $X_{source}(t)$ and the destination message $X_{dest}(t)$ are in general different, and depend on the particular design of engineered cell-to-cell communication system. For example, in the communication system utilized in our information exchange estimations, the source message $X_{source}(t)$ is a concentration of molecules of the reagent Isopropyl β-D-1-thiogalactopyranoside (IPTG) released in the transmitter cell environment, while the destination message $X_{dest}(t)$ is the level of fluorescence observed at the receiver cell [30], or equivalently the proportional concentration of Green Fluorescent Proteins (GFPs), as described in Sec. IV.

This system model and the rest of the paper are based on the following assumptions:

- The concentration of all the aforementioned molecule species is considered homogeneous at any time instant inside the cells, which corresponds to the well-stirred system assumption in chemical system modeling [24]. This assumption does not hold for the concentration of the diffusing molecules from the transmitter cell to the receiver cell in the extracellular space, which is modeled through the probability of capture by a spherical absorber under the assumption that transmitter and receiver are relatively close with respect to the receiver radius [4], as detailed below.
- The membranes of the transmitter and receiver cells separate the intracellular space from the extracellular space. The molecular species whose concentrations are $X_i(t)$ and $X_j(t)$, where $i = 1, \ldots, S_{tx}$ and $j = 1, \ldots, S_{rx}$, respectively, are considered as biological macromolecules (*e.g.*, proteins, DNA, etc.), and are confined inside the intracellular space. The molecular species whose concentrations are $X_{source}(t)$, $X_{tx}(t)$, $X_{rx}(t)$, and $X_{dest}(t)$ are considered small molecules and can cross the membranes of the transmitter and the receiver.
- Each chemical reaction in the system, expressed in general as $\mathrm{A} + \mathrm{B} \underset{\mathrm{k_r}}{\overset{\mathrm{k_f}}{\rightleftharpoons}} \mathrm{C} + \mathrm{D}$, where A, B are the reactant molecule species, C, D are the product molecule species, and k_f and k_r and the forward and reverse reaction rates, respectively (for irreversible reactions $k_r = 0$ and the backward arrow is omitted, and B and/or D can be omitted depending on the reaction), is modeled mathematically through mass action kinetics as follows [24]: $\frac{d[C](t)}{dt} = k_f[A](t)[B](t) - k_r[C](t)[D](t)$, where $[.](t)$ denotes the concentration of the molecule species as function of the time t. The same expression is valid by substituting $[D](t)$

in place of $[C](t)$. Chemical reactions are affected by noise according to the Chemical Master Equation (CME) [24], which can be computationally implemented through the Gillespie's Stochastic Simulation Algorithm (SSA) [16].

- The molecule species included in the engineered cell-to-cell communication system might be subject to degradation reactions, expressed as follows $\mathrm{A} \xrightarrow{\mathrm{k_d}} 0$, where k_d is the degradation rate. These reactions are modeled in this paper though the aforementioned mass action kinetics formulation as $\frac{d[A](t)}{dt} = -k_d[A](t)$, and their noisy behavior can be computationally simulated through SSA.
- The propagation of molecule species with concentration $X_{tx}(t)$ from the transmitter cell to the receiver cell, with concentration $X_{rx}(t)$, is realized through free diffusion in the extracellular environment, in agreement with several engineered cell-to-cell communication systems [26,28,40]. In this paper, we model this process through a mass action kinetics formulation, based on the probability of capture of a diffusing particle by a spherical absorber [4]. For this, we express the propagation as follows: $\frac{dX_{rx}(t)}{dt} = P_{cap}X_{tx}(t)$, where $P_{cap} = r_c/R$, r_c being the average radius of the receiver cell, and R the average distance between the center of the receiver cell and the membrane of the receiver cell. As a consequence, also molecule propagation between the transmitter cell and the receiver cell is affected by noise according to CME, and it can be computationally simulated through SSA.
- The source message $X_{source}(t)$ is input to the system by releasing molecules in the environment, consequently varying the concentration $X_{source}(t_0)$, where t_0 corresponds to an initial state of the system, by an amount $\overline{X}_{source}$, whose value represents the source information. This models the situation where in a lab experiment a chemical reagent is added to a cell culture in a determinate quantity [30]. The destination message $X_{dest}(t)$ is in general function of the time t, but in this paper we consider solely the information content of the maximum value $\overline{X}_{dest}$ of the destination message after the release of a message from the source. This corresponds to measuring the maximum output of the system, and it is inline with the dose-response characterization often made in experimental studies of cell-to-cell communications, such as in [34].

III. Characterizing Information Exchange Performance

In this paper, our goal is to characterize the information exchange performance of an engineered cell-to-cell communication system through the MI parameter $I(\overline{X}_{source}; \overline{X}_{dest})$, which quantifies the amount of information about the source message $\overline{X}_{source}$ that we can obtain through the knowledge of the corresponding destination message $\overline{X}_{dest}$ [11]:

$$I(\overline{X}_{source}; \overline{X}_{dest}) = H(\overline{X}_{dest}) - H(\overline{X}_{dest}|\overline{X}_{source}) , \quad (1)$$

where the expressions for the differential entropy of the destination message $H(\overline{X}_{dest})$ and the conditional entropy of the destination message given the source message $H(\overline{X}_{dest}|\overline{X}_{source})$ for an engineered cell-to-cell communication system are as follows:

$$H(\overline{X}_{dest}) = \int_{x_{dest}^{min}}^{x_{dest}^{max}} P_{\overline{X}_{dest}}(x_{dest}) \log_2 \left(P_{\overline{X}_{dest}}(x_{dest})\right) dx_{dest} , \quad (2)$$

and

$$H(\overline{X}_{dest}|\overline{X}_{source}) = \int_{x_{source}^{min}}^{x_{source}^{max}} P_{\overline{X}_{source}}(x_{source}) \int_{x_{dest}^{min}}^{x_{dest}^{max}} P_{\overline{X}_{dest}|\overline{X}_{source}}(x_{dest}|x_{source}) \cdot \log_2 \left(P_{\overline{X}_{dest}|\overline{X}_{source}}(x_{dest}|x_{source})\right) dx_{dest} dx_{source} , \quad (3)$$

where x_{dest}^{min} and x_{dest}^{max} are the minimum and maximum values of the destination message $X_{dest}(t)$ when the source message varies between x_{source}^{min} and x_{source}^{max}, $P_{\overline{X}_{source}}(x_{source})$ is the probability density of the source message for the value x_{source}, $P_{\overline{X}_{dest}}(x_{dest})$ is the probability density of the destination message for the value x_{dest}, and $P_{\overline{X}_{dest}|\overline{X}_{source}}(x_{dest}|x_{source})$ is the conditional probability density for the destination message with value x_{dest} given the source message with value x_{source}.

A. Analytical Formulation

The time evolution of an engineered cell-to-cell communication system as abstracted in Sec. II can be expressed according to the Chemical Langevin Equation (CLE) approximation as follows [15]:

$$\frac{dX_i(t)}{dt} = \sum_{m=1}^{M} V_{im} a_m(\mathbf{X}(t)) + \sum_{m=1}^{M} V_{im} \sqrt{a_m(\mathbf{X}(t))} \Gamma_m(t) , \quad (4)$$

where $X_i(t)$ and V_{im} are the i-th components of the vector $\mathbf{X}(t)$ containing all the molecule concentrations as function of the time t, defined in Sec II, and the stoichiometric vector $\mathbf{V}_m$, equal to the changes in the number of molecules for each species that the chemical reaction m operates when it occurs, respectively, and $\Gamma_m(t)$ is a white noise process for the reaction m, statistically independent from the white noise processes of other reactions. The parameter $a_m(\mathbf{X}(t))$ is called propensity function of the chemical reaction m, and it corresponds to the probability that the reaction m occurs in an infinitesimal time interval after time t, given the values in $\mathbf{X}(t)$. The propensity function $a_m(\mathbf{X}(t))$ for a chemical reaction m of the type considered in this paper is computed as follows [15]:

$$a_m(\mathbf{X}(t)) = \Omega k_m \prod_{X_i \in \mathcal{R}_m} X_i(t) , \quad (5)$$

where $\mathcal{R}_m$ is the set of reactant species for the chemical reaction m, k_m is the reaction rate, and Ω is the volume of the space that contains these reactants species, equal to the volume of the transmitter or receiver cells.

By operating an integration of the expression in (4), the destination message can be mathematically expressed as follows:

$$X_{dest}(t) = X_{dest}(t_0) + \sum_{m=1}^{M} V_{im} \int_{t_0}^{t} a_m(\mathbf{X}(\tau))d\tau + \sum_{m=1}^{M} V_{im} \int_{t_0}^{t} \sqrt{a_m(\mathbf{X}(\tau))}\Gamma_m(\tau)d\tau \,, \tag{6}$$

where $X_{dest}(t_0)$ is the value of the initial molecule concentration at t_0, which is defined above. The expression in (6) does not have a closed-form analytical solution in terms of input-output behavior, and its stochastic component has the mathematical shape of the integral of a non-stationary Gaussian process with increments correlated through the evolution of the state of the system $\mathbf{X}(\tau)$, where $\tau \in [t_0, t]$. These complex behaviors do not allow for an analytical estimation of an MI formula in a closed-form fashion. Although methods exist for the linear approximation of these stochastic components [8], these have limited applicability to systems with low molecule count, such as biological circuits [24], defined in the following. As a consequence, we motivate the utilization of methods for the stochastic simulation of the system to estimate the MI, according to the following computational approach.

B. Computational Formulation

Since the estimation of the MI expressed in (4) is in general not analytically tractable, as detailed in Sec. III-A, we adopt a computational approach based on the aforementioned SSA methodology [16] for simulating the time evolution of the engineered cell-to-cell communication system affected by noise. Based on this simulation methodology, we estimate the MI by collecting and analyzing data according to the procedure in [9,18,34], with the main difference that here we are based on a computational model rather than expensive wet lab experiments, which does not pose stringent constraints on the size of the data set that can be collected.

For each value $X_{source,i}$, $i = 0, \ldots, I$, of the source message $\overline{X}_{source}$ sampled from the range between x_{source}^{min} and x_{source}^{max}, defined here as the value below which the communication system does not have output, and the value above which the communication system does not show noticeable changes in output, respectively, we run the SSA simulation of the engineered cell-to-cell communication system. Consequently, we obtain the corresponding value $X_{dest,i}$ which will be in the range between an x_{dest}^{min} and an x_{dest}^{max}. Each SSA simulation is run independently, and starts in the same steady state that the system reaches with a source message value $\overline{X}_{source} = 0$.

The sample distributions of the destination message, $P_{\overline{X}_{dest}}(x_{dest})$ and the conditional probability density $P_{\overline{X}_{dest}|\overline{X}_{source}}(x_{dest}|x_{source})$ are obtained from histograms, which are built by dividing the range of output message values $X_{dest,i}$ in N uniform spaced bins of width $w_{\overline{X}_{dest}}$ and $w_{\overline{X}_{dest}|\overline{X}_{source}}$, respectively. The estimated differential entropy $\tilde{H}(\overline{X}_{dest})$ of the output message is obtained from the following:

$$\tilde{H}(\overline{X}_{dest}) = -\sum_{n=1}^{N} p_{\overline{X}_{dest}}(x_{dest,n}) \log_2 \left(\frac{p_{\overline{X}_{dest}}(x_{dest,n})}{w_{\overline{X}_{dest}}} \right), \tag{7}$$

where $p_{\overline{X}_{dest}}(x_{dest,n})$ is the amplitude of the histogram in the nth bin centered in $x_{dest,n}$. The same discrete form of the entropy is used to compute an estimate of the conditional entropy $P_{\overline{X}_{dest}|\overline{X}_{source}}(x_{dest}|x_{source})$. In this case a histogram of the output distribution is built for each aforementioned value of the considered discrete input concentration $X_{source,i}$. The resulting estimate is given by

$$\tilde{H}(\overline{X}_{dest}|x_{source,i}) = -\sum_{n=1}^{N} p_{\overline{X}_{dest}|\overline{X}_{source}}(x_{dest,n}|x_{source,i}) \log_2 \left(\frac{p_{\overline{X}_{dest}|\overline{X}_{source}}(x_{dest,n}|x_{source,i})}{w_{\overline{X}_{dest}|\overline{X}_{source}}} \right), \tag{8}$$

where $p_{\overline{X}_{dest}|\overline{X}_{source}}(x_{dest,n}|x_{source,i})$ is the amplitude of the histogram in the nth bin centered in $x_{dest,n}$ for the considered value of input concentration $x_{source,i}$. It is worth observing that, in contrast to digital communication systems, in the context of a cell-to-cell communication system the conditional entropy is not independent from the value of the input symbol [14]. Hence, in order to estimate the MI we need to average over the distribution of the input concentration samples.

Finally, we estimate the MI for a given value of the probability distribution $p_{\overline{X}_{source}}(x_{source,i})$, $i = 0, \ldots, I$ of the source message as

$$\tilde{I}_{p_{\overline{X}_{source}}}(\overline{X}_{dest}, \overline{X}_{source}) = \tilde{H}(\overline{X}_{dest}) - \tilde{H}(\overline{X}_{dest}|\overline{X}_{source}) \,, \tag{9}$$

where the conditional entropy is found by averaging (8) over the source message probability distribution as follows:

$$\tilde{H}(\overline{X}_{dest}|\overline{X}_{source}) = \sum_{i=1}^{I} \tilde{H}(\overline{X}_{dest}|x_{source,i}) \, p_{\overline{X}_{source}}(x_{source,i}) \,. \tag{10}$$

The information capacity of the engineered cell-to-cell communication system can be found as the maximum of the MI $\tilde{I}_{p_{\overline{X}_{source}}}(\overline{X}_{dest}, \overline{X}_{source})$ with respect to a varying probability distribution $p_{\overline{X}_{source}}(x_{source,i})$, $i = 0, \ldots, I$ of the source message values. As detailed in Sec. V, in this paper we show how this MI varies for the case study described in the following when different probability distributions of the source message values are considered. A full-fledged optimization problem formulation to estimate the information capacity, which should also take into account factors related to the optimal sampling of the input messages, is not within the scope of this paper, and will be considered in future work.

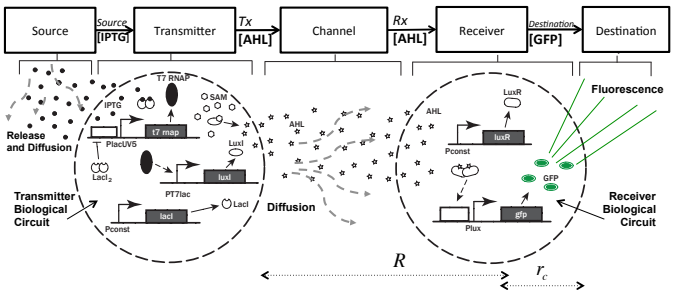

Fig. 2: Scheme of the LuxR-LuxI-based cell-to-cell communication system.

IV. Case Study: A LuxR-LuxI-based Engineered Cell-to-cell Communication System

In Fig. 2 we show the specific engineered cell-to-cell communication system considered in this paper as a case study for the performance characterization methodology detailed in Sec. II. In this system, the source message value $\overline{X}_{source}$ corresponds to a concentration of the chemical reagent IPTG (*Source* **[IPTG]**) released in the transmitter cell environment. A series of chained chemical reactions inside the transmitter, which together compose a biological circuit, defined in the following, modulates accordingly the concentration of Acyl Homoserine Lactone (AHL) (*Tx* **[AHL]**), which are small molecules, as defined in Sec. II. AHL propagates through diffusion between the transmitter cell and the receiver cell, resulting in a concentration (*Rx* **[AHL]**) at the receiver. According to this concentration value, the chemical reactions of the receiver's biological circuit modulate the concentration of GFP molecules (*Destination* **[GFP]**). The GFP concentration is also proportional to the fluorescence that can be observed from the extracellular environment [30]. The maximum value of GFP concentration after the release of IPTG at the source corresponds to the destination message value $\overline{X}_{dest}$.

A. Biological Circuit Elements

A biological circuit is a programmable network of *genes* that interact with each other through *chemical reactions*, resulting in the implementation of a specific biological function [24]. In particular, as shown in Fig. 3, a gene is composed of an *operator region* (O_R), a *promoter region* (P_R), and a *coding sequence*. Most genes are a stretch of DNA that codes for a *protein* molecule, a sequence of amino acids, expressed from the gene through the fundamental processes of *transcription* and *translation*. Protein expression can be up or down-regulated by a *transcription factor* protein *In*, *activator* (a) or *repressor* (b), respectively. When the gene expresses proteins independently from transcription factors, it is said to have a *constitutive* promoter (Pconst in Fig. 2). Protein expression is based on [24]:

- **Transcription** is initiated by the enzyme (a specific type of protein) *RNA polymerase (RNAP)* that binds to the promoter region of the considered gene, starting the production of the *messenger RNA (mRNA)* molecules. These latter molecules are used to carry the genetic information encoded in the coding sequence of the gene to the *ribosome*, the protein assembly machinery. The ability of RNAP to bind to promoter site can be either enhanced or impeded by the aforementioned activators or repressors, respectively.
- **Repression** is present when repressors obstruct the binding sites of the promoter region and down-regulate the transcription of the subsequent coding sequence by reducing RNAP binding rate.
- **Activation** happens if activators bind to the operator region near the promoter site up-regulating the transcription of the subsequent coding sequence by increasing the RNAP binding rate.
- **Translation** is performed through the ribosomes, which are able to recognize and bind to the mRNA molecules by means of *Ribosome Binding Sites (RBSs)*, special sequences of nucleotides in the mRNA strand. Once a ribosome binds to the RBS of an mRNA molecule, it completes the synthesis of the corresponding protein by assembling together the component amino acids.

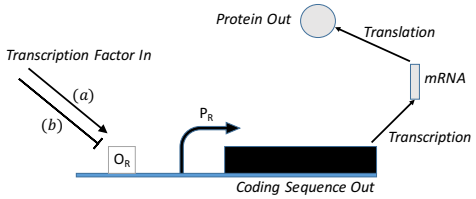

Fig. 3: Gene expression: (a) Activation (↓), (b) Repression (⊥).

B. Biological Circuits in the LuxR-LuxI-based System

The biological circuits at the transmitter cell and receiver cell of our case study system shown in Fig. 2 are derived from the artificial sender and receiver circuits presented in [30], where they are implemented and experimentally characterized, albeit not in terms of information exchange performance. These biological circuits contain the following genes and chemical reactions.

The transmitter cell contains genes that include a promoter that binds exclusively to a particular type of virus-derived RNAP, the T7 RNAP, which is coded by another gene. The transcription of this latter gene is controlled by the PlacUV5 promoter, and it is repressed by the transcription factor $LacI_2$, which results from a binding chemical reaction between two LacI proteins. The LacI protein is synthesized from a gene controlled by the constitutive promoter Pconst. When a concentration of IPTG molecules is present in the transmitter cell environment, its value modulates the inhibition of the repression of T7 RNAP synthesis, because IPTG molecules bind to $LacI_2$ (dimer), preventing its function as transcription factor. After transcription and translation, the T7 RNAP can bind to the promoter PT7lac, which controls the expression of the LuxI protein. The LuxI protein can synthesize the AHL small molecules by reacting with S-AdenosylMethionine (SAM) molecules, which are abundant small molecules in the transmitter cell environment.

The biological circuit at the receiver cell includes a gene that constitutively expresses the protein LuxR. Through a series of two chemical reactions, LuxR proteins form a complex with the AHL molecules, and two of them react to form a dimer, as shown in Fig. 2. The LuxR-AHL dimer, whose concentration

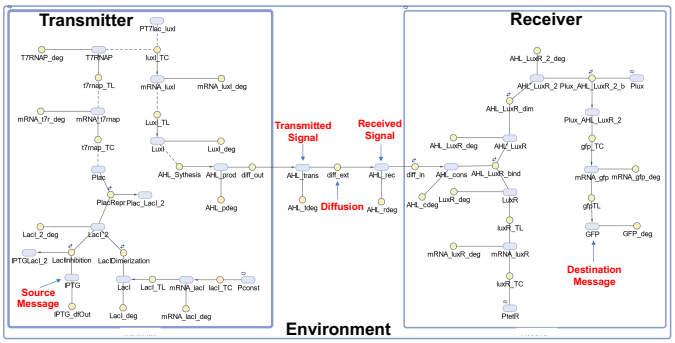

Fig. 4: A diagram view of the Matlab Simbiology model of the LuxR-LuxI-based cell-to-cell communication system.

is modulated by the concentration of AHL molecules in the receiver cell environment, can bind to the operator site of the promoter Plux, and modulate through activation the expression GFPs. In this study, the concentration of GFP at the receiver cell is the quantifiable destination message of the cell-to-cell communication system.

C. Computational Model

In order to perform the computational estimation of the information exchange performance detailed in Sec. III-B, we developed a computational model of the engineered cell-to-cell communication system described above. This model contains the description of all the chemical reactions included in the system, which are summarized in Table I according to the mass action kinetics formulation described in Sec. II.

Our computational model, implemented in the Matlab Simbiology environment, is schematically shown in Fig. 4, where each molecule species is represented by a light blue oval, and each chemical reaction by a yellow circle. Genes are represented as molecules by the name of their respective promoter (e.g. Plux, PT7lac, etc.). The model includes concentration values for these genes, which is in agreement with the biological reality in terms of copy number of DNA vectors where these genes are hosted [24]. Directed edges connect chemical reactions with products, while normal edges connect reactants with the respective chemical reactions where they participate. This model takes into account each single reaction of transcription, translation, degradation, complex formation, protein expression, and diffusion, as described in Sec.II. The model is composed of three compartments, the **Transmitter** compartment, the **Receiver** compartment, and the **Environment** compartment, according to the compartment definition of Simbiology, and represented in the diagram as a rectangular box. The values of the kinetic constants used to implement the mass action kinetics reactions, which are shown in Fig. 4 and expressed in Table I, are listed in Table II. The Simbiology environment allows to perform SSA-based simulations [16] and obtain the results detailed in Sec. V.

V. Numerical Results

In this section, we present the results obtained from the simulations of the end-to-end LuxR-LuxI cell signaling system model given in Fig. 4. These simulations have been realized by using the computational model presented in Sec. IV-C.

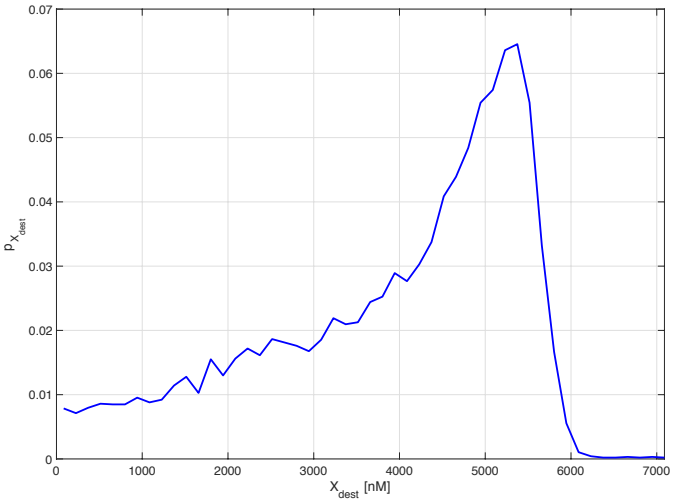

Fig. 5: Estimate of the output distribution given uniform input distribution having support between 10^6 nM and 10^7 nM.

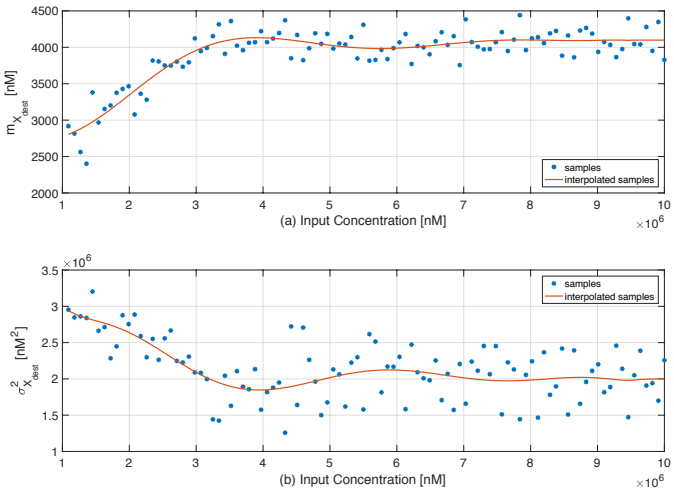

Fig. 6: Estimated average (a) and variance (b) of the output concentration.

In Fig. 5, we show the estimated distribution of the maximum GFP output concentration obtained when IPTG with uniform concentration between 10^6 nM and 10^7 nM is applied at the input. From the figure it can be observed that the estimated distribution has a peak close to the maximum of the observed GFP output, which is around $7.1 \cdot 10^3$ nM.

In order to better understand the input/output behavior of the system, we estimated the average $m_{X_{dest}}$ and the variance $\sigma^2_{X_{dest}}$ from the GFP samples obtained at a given fixed value of the input IPTG concentration. The results are shown in Fig. 6 (a) and 6 (b) for the average and the variance, respectively. It can be observed that for values of the input IPTG concentrations below $3 \cdot 10^6$ nM there is a linear increase of the average and a linear decrease of the variance. For values higher that $3 \cdot 10^6$ there is a saturation of the measured average value and the associated variance that remains almost constant up to 10^7, which is the maximum value of the IPTG concentration at the input.

The goal of running these initial simulations was to estimate

TABLE I: List of reactions included in the LuxR-LuxI-based engineered cell-to-cell communication system expressed in terms of mass action kinetics. Tx, Env, and Rx denote the volume of the transmitter cell, environment, and receiver cell, respectively, necessary for rate conversions in reactions that include molecules that propagate between different compartments.

Transmitter
$\frac{d[Plac]}{dt} = (1/Tx) * (-((bPlac * [LacI_2] * [Plac]) * Tx - (ubPlac * [Plac\_LacI\_2]) * Tx))$
$\frac{d[mRNA\_t7rnap]}{dt} = (1/Tx) * (((ts\_t7rnap * [Plac]) * Tx) - ((dm\_mRNA\_t7rnap * [mRNA_t7rnap]) * Tx))$
$\frac{d[mRNA\_luxI]}{dt} = (1/Tx) * (((ts\_luxI * [PT7lac_luxI] * [T7RNAP]) * Tx) - ((dm\_mRNA\_luxI * [mRNA\_luxI]) * Tx))$
$\frac{d[AHL\_prod]}{dt} = (1/Tx) * (((sAHL * [LuxI]) * Tx) - ((dAHL * [AHL_prod]) * Tx) - ((dfAHL * [AHL_prod]) * Tx))$
$\frac{d[IPTG]}{dt} = (1/Tx) * (-(dfIPTG * [IPTG] * Tx) - ((bIPTGLacI\_2 * [IPTG] * [LacI\_2]) * Tx - (ubIPTGLacI * [IPTGLacI\_2]) * Tx))$
$\frac{d[LacI\_2]}{dt} = (1/Tx) * (((bLacI * [LacI] * [LacI]) * Tx - (ubLacI\_2 * [LacI_2]) * Tx) - ((bPlac * [LacI_2] * [Plac]) * Tx - (ubPlac * [Plac\_LacI\_2]) * Tx) - ((bIPTGLacI\_2 * [IPTG] * [LacI\_2]) * Tx - (ubIPTGLacI * [IPTGLacI\_2]) * Tx) - ((dLacI\_2 * [LacI\_2]) * Tx))$
$\frac{d[LacI]}{dt} = (1/Tx) * (((tl\_lacI * [mRNA_lacI]) * Tx) - 2((bLacI * [LacI] * [LacI]) * Tx - (ubLacI\_2 * [LacI_2]) * Tx) - ((dLacI * [LacI]) * Tx))$
$\frac{d[IPTGLacI\_2]}{dt} = (1/Tx) * ((bIPTGLacI\_2 * [IPTG] * [LacI\_2]) * Tx - (ubIPTGLacI * [IPTGLacI\_2]) * Tx)$
$\frac{d[T7RNAP]}{dt} = (1/Tx) * (((tl\_t7rnap * [mRNA\_t7rnap]) * Tx) - ((dT7RNAP * [T7RNAP]) * Tx))$
$\frac{d[LuxI]}{dt} = (1/Tx) * (((tl\_luxI * [mRNA\_luxI]) * Tx) - ((dLuxI * [LuxI]) * Tx))$
$\frac{d[Plac\_LacI\_2]}{dt} = (1/Tx) * ((bPlac * [LacI_2] * [Plac]) * Tx - (ubPlac * [Plac\_LacI\_2]) * Tx)$
$\frac{d[mRNA\_lacI]}{dt} = (1/Tx) * (-((dmLacI * [mRNA_lacI]) * Tx) - ((tl\_lacI * [mRNA_lacI]) * Tx) + ((ts\_lacI * [Pconst]) * Tx))$
Environment
$\frac{d[AHL\_trans]}{dt} = (1/Env) * (((dfAHL * [AHL_prod]) * Tx) - ((dfAHL\_env * [AHL\_trans]) * Env) - ((dAHL * [AHL\_trans]) * Env))$
$\frac{d[AHL\_rec]}{dt} = (1/Env) * (((dfAHL\_env * [AHL\_trans]) * Env) - ((dfAHL * [AHL\_rec]) * Env - (dfAHL * [AHL\_cons]) * Rx) - ((dAHL * [AHL\_rec]) * Env))$
Receiver
$\frac{d[mRNA\_LuxR]}{dt} = (1/Rx) * (((ts\_luxR * [PtetR]) * Rx) - ((tl\_luxR * [mRNA\_luxR]) * Rx) - ((dm\_mRNA\_luxR * [mRNA\_luxR]) * Rx))$
$\frac{d[LuxR]}{dt} = (1/Rx) * (((tl\_luxR * [mRNA\_luxR]) * Rx) - ((bAHL\_LuxR * [LuxR] * [AHL\_cons]) * Rx - (ub\_AHL\_LuxR * [AHL\_LuxR]) * Rx) - ((dLuxR * [LuxR]) * Rx))$
$\frac{d[AHL\_LuxR]}{dt} = (1/Rx) * (((bAHL\_LuxR * [LuxR] * [AHL\_cons]) * Rx - (ub\_AHL\_LuxR * [AHL\_LuxR]) * Rx) - 2((bAHL\_LuxR\_2 * [AHL\_LuxR] * [AHL\_LuxR]) * Rx - (ubAHL\_LuxR\_2 * [AHL\_LuxR\_2]) * Rx) - ((dAHL\_LuxR * [AHL\_LuxR]) * Rx))$
$\frac{d[mRNA\_gfp]}{dt} = (1/Rx) * (-((tl_gfp * [mRNA\_gfp]) * Rx) - ((dm\_mRNA\_gfp * [mRNA\_gfp]) * Rx) + ((ts_gfp * [Plux\_AHL\_LuxR\_2]) * Rx))$
$\frac{d[GFP]}{dt} = (1/Rx) * (((tl_gfp * [mRNA\_gfp]) * Rx) - ((dGFP * [GFP]) * Rx))$
$\frac{d[AHL\_LuxR\_2]}{dt} = (1/Rx) * (((bAHL\_LuxR\_2 * [AHL\_LuxR] * [AHL\_LuxR]) * Rx - (ubAHL\_LuxR\_2 * [AHL\_LuxR\_2]) * Rx) - ((dAHL\_LuxR\_2 * [AHL\_LuxR\_2]) * Rx) - ((bPlux\_AHL\_LuxR\_2 * AHL\_LuxR\_2 * Plux) * Rx - (ubPlux\_AHL\_LuxR\_2 * [Plux\_AHL\_LuxR\_2]) * Rx))$
$\frac{d[Plux\_AHL\_LuxR\_2]}{dt} = (1/Rx) * (((bPlux\_AHL\_LuxR\_2 * AHL\_LuxR\_2 * [Plux]) * Rx - (ubPlux\_AHL\_LuxR\_2 * [Plux\_AHL\_LuxR\_2]) * Rx) - ((ts_gfp * [Plux\_AHL\_LuxR\_2]) * Rx))$
$\frac{d[AHL\_cons]}{dt} = (1/Rx) * (-((bAHL\_LuxR * [LuxR] * [AHL\_cons]) * Rx - (ub\_AHL\_LuxR * [AHL\_LuxR]) * Rx) + ((dfAHL * [AHL\_rec]) * Env - (dfAHL * [AHL\_cons]) * Rx) - ((dAHL * [AHL\_cons]) * Rx))$

TABLE II:

List of the parameter values used in the computational model of the LuxR-LuxI-based engineered cell-to-cell communication system, with reference to the mass action kinetics expressions in Table I.

Parameter	Description	Value	Unit	Reference
ts_t7rnap	transcription of t7rnap	1.017	1/min	[6]
ts_luxI	transcription of luxI	4.199	1/min	[6]
ts_luxR	transcription of luxR	3.457	1/min	[6]
ts_gfp	transcription of gfp	3.75	1/min	[6]
ts_lacI	transcription of lacI	2.493	1/min	[6]
tl_t7rnap	translation of t7rnap	1.356	1/min	[38]
tl_luxI	translation of luxI	5.587	1/min	[38]
tl_luxR	translation of luxR	4.608	1/min	[38]
tl_gfp	translation of gfp	5	1/min	[38]
tl_lacI	translation of lacI	3.324	1/min	[38]
dLacI, dLacI_2, dIPTGLacI_2	degradation of LacI, LacI_2, IPTGLacI_2	0.2	1/min	[33]
dmLacI	degradation of LacI mRNA	0.462	1/min	[33]
dm_mRNA_*; *= t7rnap, luxI, luxR, gfp	degradation of mRNA for t7rnap, luxI, luxR, or gfp	0.347	1/min	[31]
dT7RNAP	degradation of T7RNAP	0.3	1/min	[7]
dLuxI	degradation of LuxI	0.027	1/min	[5]
dLuxR, dAHL_LuxR, dAHL_LuxR_2	degradation of LuxR, AHL_LuxR, and AHL_LuxR_2	0.002	1/min	[39]
dAHL	degradation of AHL	0.057	1/min	[5]
dGFP	degradation of GFP	0.0692	1/min	[5]
bLacI	binding of LacI - dimerization	50	1/(min*nM)	[33]
ubLacI_2	unbinding of LacI - dimerization	0.01	1/min	[33]
bPlac_LacI_2	binding of the LacI dimer to the dna	960	1/(min*nM)	[33]
ubLacI_2_Plac	unbinding of LacI dimer from dna	2.4	1/min	[33]
bIPTGLacI_2	binding of LacI_2 and IPTG	6.00E-04	1/(min*nM)	[21]
ubIPTGLacI	unbinding of LacI and IPTG	0.492	1/min	[21]
bAHL_LuxR	association rate of LuxR to AHL	0.1	1/(min*nM	[39]
ubAHL_LuxR, ubdna_AHL_LuxR_2	unbinding of AHL from LuxR and AHL_LuxR_2 from dna	10	1/min	[39]
bAHL_LuxR_2, bdna_AHL_LuxR_2	binding of AHL_LuxR - dimerization and dna binding	0.05	1/(min*nM)	[39]
ubAHL_LuxR_2	unbinding of AHL + LuxR dimer	1	1/min	[39]
sAHL	AHL Synthesis rate	0.04	1/min	[39]
dfIPTG	diffusion rate of IPTG into the cell	0.92	1/min	[32]
dfAHL	diffusion rate of AHL	2	1/min	[13]
dfAHL_env	diffusion rate of AHL in the environment	.45/(5+.45)=.0826	1/min	[4]
vCell	volume of *E. coli*	8.00E-16	L	[32]
vEnv	volume of the Environment	100	L	>> vCell
rCell	radius of *E. coli* cell body	0.45	μm	[17]
dtcCell	distance between cells	30	μm	[10]

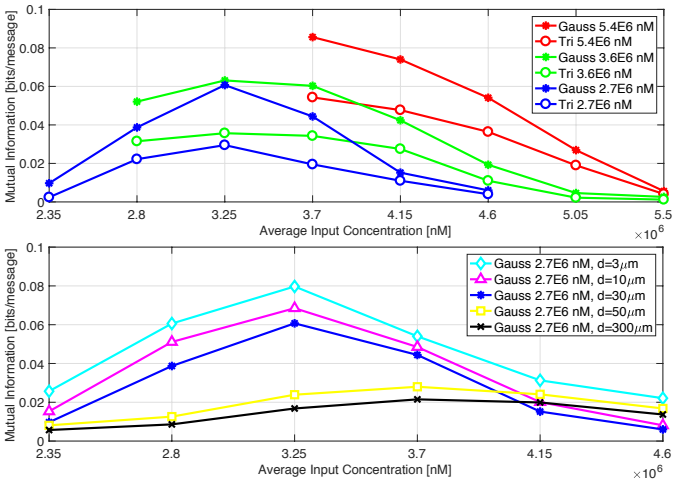

Fig. 7: Mutual Information versus average value of the input concentration for Gaussian and triangular probability density functions with different concentration supports (upper), and varying distance between cells (lower).

the GFP output range of the LuxR-LuxI computational model. Figures 5 and 6 suggest that the information channel is linear until up to an input concentration around $3 \cdot 10^6$. This means that even if we increase the concentration of the imput distribution there is a saturation effect that limits the output value, thus emphasizing a nonlinear behavior of the end-to-end LuxR-LuxI cell signaling system.

By taking into account the saturation effect introduced by the channel, in the following we present the results obtained from the computation of the MI. As illustrated in Sec. III-B, the MI is evaluated by replacing (7) and (10) into (9). It is well known that the search over the space of all the input distributions allows to find the one that maximizes the mutual information and gives the capacity of the channel. However, due to the lack of analytical expressions, and the need to study additional factors related to the optimal sampling of the input messages, a full-fledged optimization problem formulation to estimate the information capacity is not within the scope of this paper. Here, we resort to the use of two arbitrary, yet reasonable, distributions to evaluate how the MI is affected by the choice of the input distribution. The first considered distribution is defined by a Gaussian shape and the second distribution by a triangular shape, the latter being normalized to have unitary area. Fig. 7 reports the results of mutual information measured in bit/message as a function of the average input concentration for the two considered input distributions. The support is the range of values spanned by the input concentration, and in the results reported in Fig. 7 (upper) we considered $5.4 \cdot 10^6$ nM, $3.6 \cdot 10^6$ nM, and $2.7 \cdot 10^6$ nM. Moreover, in Fig. 7 (lower) we show the results for a Gaussian-distributed input with support of $2.7 \cdot 10^6$ nM for different distances between cells, ranging from one order of magnitude less to one order of magnitude more than the 30 μm in Table II. Since in the case of the Gaussian distribution the support is infinite by definition, we truncated it to a finite value by rectangular windowing. The results reported in the figure show that at low values of the average input concentration there is an increase of the mutual information for increasing average values. For higher input average values, the MI starts decreasing due to the saturation effects associated to the nonlinearity of the channel. As expected, the greater the support of the input distribution, the higher is the mutual information. It is worth observing that the maximum value of estimated mutual information is in the order of 0.1 bit/message, from which we can conclude that the considered end-to-end LuxR-LuxI-based cell-to-cell communication system is highly corrupted by noise. This encourages further investigation into techniques to mitigate the noise impairments, perhaps inspired by nature, such as that discussed in the experimental study in [34].

VI. Conclusion

In this paper, we proposed a computational approach to characterize information exchange in engineered cell-to-cell communication systems. Although these systems have been experimentally demonstrated for various applications, ranging from cancer treatment to tissue engineering, approaches to characterize them in terms of communication performance and their dependence on design parameters have been very limited. Our method, based on based on stochastic simulation of biochemical models estimation of information-theoretic parameters from sample distributions, will potentially fill this gap, and provide quantifiable metrics to compare and optimize these systems starting from the design phase, before expensive trial-and-error experiments.

In particular, in this paper we abstracted the main features of engineered cell-to-cell communication systems, and demonstrated through an analytical formulation that these systems do not have closed-form analytical solutions for the characterization of their communication performance. We detailed a methodology based on chemical stochastic simulations and applied it to characterize the communication performance of a realistic synthetic biology design. A computational model, built using the Simbiology software, allowed us to track the evolution of the state of the system through time during the propagation of information. By using the sample distributions generated from the simulations, we were able to estimate the mutual information. Additionally, we studied the mutual information behavior as a function of the average input of the system considering two different distributions, which were also parameterized by their support, *i.e.*, the range spanned by the input values. We showed that optimization is possible by changing input distributions. Moreover, we observed that the input/output characteristic of the system presents a saturation that destroys the information for high level of the input concentration, leading to a decrease of the mutual information for high average values of the input concentration.

Our research suggests that, despite complexity, turning to the biological domain to engineer communication systems is promising. A theoretical foundation for more comprehensive characterizations of cell signaling systems in terms of communication performance and design parameters will soon allow

for faster and more reliable forward engineering of robust communication systems in the biological environment, where communication engineers will work with synthetic biologists by providing standardized metrics to engineer, compare, and optimize these systems.

ACKNOWLEDGMENT

This paper is based upon work supported by the US National Science Foundation Research Experiences for Undergraduates (REU) through grant MCB-1449014, the Nebraska Center for Integrated Biomolecular Communication (NIH National Institutes of General Medical Sciences P20-GM113126), and the University of Nebraska-Lincoln Ronald E. McNair Scholars Program.

REFERENCES

[1] I. F. Akyildiz, J. M. Jornet, and M. Pierobon, "Nanonetworks: a new frontier in communications," *Communications of the ACMs*, vol. 54, no. 11, pp. 84–89, Nov. 2011.

[2] I. F. Akyildiz, M. Pierobon, S. Balasubramaniam, and Y. Koucheryavy, "The internet of bio-nano things," *IEEE Communications Magazine*, vol. 53, no. 3, pp. 32–40, March 2015.

[3] S. Basu, Y. Gerchman, C. Collins, F. Arnold, and R. Weiss, "A synthetic multicellular system for programmed pattern formation," *Nature*, vol. 434, pp. 1130–1134, 2005.

[4] H. C. Berg, "Random walks in biology," 1993.

[5] Y. Boada, A. Vignoni, and J. Pico, "Promoter and transcription factor dynamics tune protein mean and noise strength in a quorum sensing-based feedback synthetic circuit," *bioRxiv*, 2017. [Online]. Available: http://www.biorxiv.org/content/early/2017/02/06/106229

[6] H. Bremer and P. P. Dennis, "Modulation of Chemical Composition and Other Parameters of the Cell by Growth Rate," *Escherichia coli and Salmonella: cellular and molecular biology*, vol. 2, no. 122, pp. 1527–1542, 1987. [Online]. Available: http://ctbp.ucsd.edu/qbio/beemer96.pdf

[7] Y. Cao, M. D. Ryser, S. Payne, B. Li, C. V. Rao, and L. You, "Collective Space-Sensing Coordinates Pattern Scaling in Engineered Bacteria," *Cell*, vol. 165, no. 3, pp. 620–630, 2016.

[8] L. Cardelli, M. Kwiatkowska, and L. Laurenti, "Stochastic analysis of chemical reaction networks using linear noise approximation," *Biosystems*, vol. 149, pp. 26 – 33, 2016.

[9] R. Cheong, A. Rhee, C. Wang, I. Nemenman, and A. Levchenko, "Information transduction capacity of noisy biochemical signaling networks," *Science*, vol. 334, pp. 354–358, 2011.

[10] H. Cho, H. Jönsson, K. Campbell, P. Melke, J. W. Williams, B. Jedynak, A. M. Stevens, A. Groisman, and A. Levchenko, "Self-organization in high-density bacterial colonies: Efficient crowd control," *PLoS Biology*, vol. 5, no. 11, pp. 2614–2623, 2007.

[11] T. M. Cover and J. A. Thomas, *Elements of Information Theory, 2nd Edition*. Wiley, 2006.

[12] N. Farsad, H. B. Yilmaz, A. Eckford, C.-B. Chae, and W. Guo, "A comprehensive survey of recent advancements in molecular communication," *IEEE Communications Surveys & Tutorials*, vol. 18, no. 3, pp. 1887–1919, Third Quarter 2016.

[13] J. Garcia-Ojalvo, M. B. Elowitz, and S. H. Strogatz, "Modeling a synthetic multicellular clock: repressilators coupled by quorum sensing." *Proceedings of the National Academy of Sciences of the United States of America*, vol. 101, no. 30, pp. 10 955–60, 2004. [Online]. Available: http://www.pnas.org/content/101/30/10955.full

[14] H. Ghourchian, G. Aminian, A. Gohari, M. Mirmohseni, and M. Nasiri-Kenari, "On the capacity of a class of signal-dependent noise channels," *arXiv preprint arXiv:1702.03590*, 2017.

[15] D. T. Gillespie, "The chemical langevin equation," *Journal of Chemical Physics*, vol. 113, no. 1, pp. 297–306, Jul. 2000.

[16] ——, "Stochastic simulation of chemical kinetics," *Annual Review of Physical Chemistry*, vol. 58, pp. 35–55, May 2007.

[17] J. Hu, M. Yang, G. Gompper, and R. G. Winkler, "Soft Matter Modelling the mechanics and hydrodynamics of swimming E. coli," *Soft Matter*, vol. 11, no. 40, pp. 7843–8020, 2015.

[18] A. Levchenko and I. Nemenman, "Cellular noise and information transmission," *Current Opinion in Biotechnology*, vol. 28, pp. 156–164, 2014.

[19] A. Marcone, M. Pierobon, and M. Magarini, "A biological circuit design for modulated parity-check encoding in molecular communication," in *Proceedings of the IEEE International Conference on Communications (ICC)*, May 2017.

[20] ——, "A parity check analog decoder for molecular communication based on biological circuits," in *Proceedings of the IEEE International Conference on Computer Communications (INFOCOM)*, May 2017.

[21] N. Martyushenko, S. H. Johansen, C.-M. Ghim, and E. Almaas, "Hypothetical biomolecular probe based on a genetic switch with tunable symmetry and stability." *BMC systems biology*, vol. 10, no. 1, p. 39, 2016.

[22] D. B. Menendez, V. R. Senthivel, and M. Isalan, "Sender-receiver systems and applying information theory for quantitative synthetic biology," *Curr Opin Biotechnol*, vol. 31C, pp. 101–107, March 2015.

[23] L. Morsut, K. T. Roybal, X. Xiong, R. M. Gordley, S. M. Coyle, M. Thomson, , and W. A. Lim, "Engineering customized cell sensing and response behaviors using synthetic notch receptors," *Cell*, vol. 164, no. 4, pp. 780–791, February 2016.

[24] C. J. Myers, *Engineering genetic Circuits*. Chapman & Hall, 2009.

[25] D. L. Nelson and M. M. Cox, *Lehninger Principles of Biochemistry*, 4th ed. W.H. Freeman, 2005.

[26] M. E. Ortiz and D. Endy, "Engineered cell-cell communication via dna messaging," *Journal of Biological Engineering*, vol. 6, no. 16, 2012.

[27] S. Payne and L. You, "Engineered Cell-Cell Communication and Its Applications." *Advances in biochemical engineering/biotechnology*, 2013.

[28] ——, "Engineered cell-cell communication and its applications," *Adv Biochem Eng Biotechnol*, vol. 146, pp. 97–121, 2014.

[29] M. Pierobon, "A systems-theoretic model of a biological circuit for molecular communication in nanonetworks," *Nano Communication Networks (Elsevier)*, vol. 5, no. 1-2, pp. 25–34, March-June 2014.

[30] T. Ramalho, A. Meyer, A. Mückl, K. Kapsner, U. Gerland, and F. C. Simmel, "Single Cell Analysis of a Bacterial Sender-Receiver System," *PLOS ONE*, vol. 11, no. 1, p. e0145829, 2016. [Online]. Available: http://dx.plos.org/10.1371/journal.pone.0145829

[31] C. Roberts, K. L. Anderson, E. Murphy, S. J. Projan, W. Mounts, B. Hurlburt, M. Smeltzer, R. Overbeek, T. Disz, and P. M. Dunman, "Characterizing the effect of the Staphylococcus aureus virulence factor regulator, SarA, on log-phase mRNA half-lives," *Journal of Bacteriology*, vol. 188, no. 7, pp. 2593–2603, 2006.

[32] M. Stamatakis and N. V. Mantzaris, "Comparison of deterministic and stochastic models of the lac operon genetic network," *Biophysical Journal*, vol. 96, no. 3, pp. 887–906, 2009.

[33] M. Stamatakis and K. Zygourakis, "Deterministic and stochastic population-level simulations of an artificial lac operon genetic network." *BMC bioinformatics*, vol. 12, no. 1, p. 301, 2011.

[34] R. Suderman, J. A. Bachman, A. Smith, P. K. Sorger, and E. J. Deeds, "Fundamental trade-offs between information flow in single cells and cellular populations," *PNAS*, vol. 114, no. 22, pp. 73–85, May 2017.

[35] A. Tasmir, J. Tabor, and C. Voigt, "Robust multicellular computing using genetically encoded nor gates and chemical 'wires'," *Nature*, vol. 469, pp. 212–215, 2011.

[36] P. J. Thomas and A. W. Eckford, "Capacity of a simple intercellular signal transduction channel," *IEEE Transactions on Information Theory*, vol. 62, no. 12, pp. 7358–7382, December 2016.

[37] B. D. Unluturk, A. O. Bicen, and I. F. Akyildiz, "Genetically engineered bacteria-based biotransceivers for molecular communication," *IEEE Trans. on Communications*, vol. 63, no. 4, pp. 1271–1281, 2015.

[38] U. Vogel and K. F. Jensen, "The RNA chain elongation rate in Escherichia coli depends on the growth rate," *Journal of Bacteriology*, vol. 176, no. 10, pp. 2807–2813, 1994.

[39] M. Weber and J. Buceta, "Dynamics of the quorum sensing switch: stochastic and non-stationary effects." *BMC systems biology*, vol. 7, p. 6, 2013.

[40] R. Weiss and T. Knight, "Engineered communications for microbial robotics," *Lect Notes Comput Sci*, vol. 2054, pp. 1–16, 2001.

[41] H. Ye and M. Fussenegger, "Synthetic therapeutic gene circuits in mammalian cells," *FEBS Letters*, vol. 588, no. 15, pp. 2537–2544, August 2014.

[42] L. You, R. Cox, R. Weiss, and F. Arnold, "Programmed population control by cell-cell communication and regulated killing," *Nature*, vol. 428, pp. 868–871, 2004.